Analytica Chimica Acta 1245 (2023) 340828

Contents lists available at ScienceDirect

Analytica Chimica Acta

journal homepage: www.elsevier.com/locate/aca

Fluorescent sensor based on solid-phase extraction with negligible depletion: A proof-of-concept study with amines as analytes

Miao Zhang [a], Rana Dalapati [b,c], Jiangfan Shi [b,c], Chenglong Liao [a], Qingyun Tian [a], Chuanyi Wang [a], Xiaomei Yang [b], Shuai Chen [e,**], Marc D. Porter [b,d,***], Ling Zang [b,c,*]

[a] School of Environmental Science and Engineering, Shaanxi University of Science and Technology, Shaanxi, Xi'an, 710021, China
[b] Nano Institute of Utah, University of Utah, Salt Lake City, UT, 84112, USA
[c] Department of Materials Science and Engineering, University of Utah, Salt Lake City, UT, 84112, USA
[d] Department of Chemical Engineering, University of Utah, Salt Lake City, UT, 84112, USA
[e] Jiangxi Engineering Laboratory of Waterborne Coating, Jiangxi, Nanchang, 330013, China

HIGHLIGHTS

- A novel fluorescent sensor, namely F-SPE, is developed from solid-phase extraction (SPE) disk modified with perylene diimide (PDI) fluorophore.
- F-SPE demonstrates effective detection of aniline and Kanamycin, with limit of detection (LOD) down to 67 and 32 nM, respectively.
- The sensing mechanism is based on the donor-acceptor fluorescence quenching of PDI by amines.
- The high detection sensitivity of F-SPE is mainly due to the high porosity of SPE substrate that helps concentrate the analytes from solution phase.
- F-SPE significantly simplifies the analysis process by eliminating the need to precisely meter the sample volume.

GRAPHICAL ABSTRACT

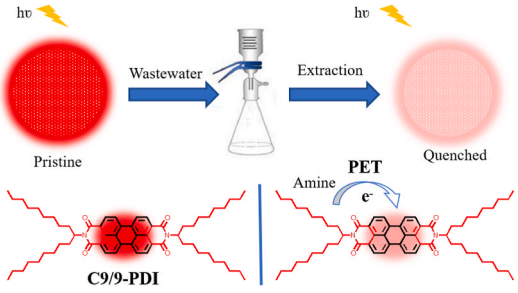

ARTICLE INFO

Handling Editor: Prof Lin Yuehe

Keywords:
Perylene diimide
Fluorescent sensor
Organic amine
Solid-phase extraction
Water pollutant detection

ABSTRACT

This paper describes the development and proof-of-concept testing of an easy-to-use trace analysis technique, namely F-SPE, by coupling fluorescent sensor with solid phase extraction (SPE). F-SPE is a two-step methodology that concentrates an analyte from a liquid sample onto a fluorophore-modified membrane and measures the amount of analyte from the extent the extracted analyte quenches the emission of the fluorophore. By applying the principle of negligible depletion (ND) intrinsic to SPE, the procedure of F-SPE for analyzing a sample can be markedly simplified while maintaining the ability to detect analytes at low limits of detection (LOD). The merits of this approach are demonstrated by impregnating a SPE membrane with a perylene diimide (PDI) fluorophore, N,N′-di(nonyldecyl)-perylene-3,4,9,10-tetracarboxylic diimide (C9/9-PDI), for the low-level detection of organic amines (e.g., aniline) and amine-containing drugs (e.g., Kanamycin). The sensing mechanism is based on the

* Corresponding author. Nano Institute of Utah, University of Utah, Salt Lake City, UT, 84112, USA.
** Corresponding author.
*** Corresponding author. Department of Chemical Engineering, University of Utah, Salt Lake City, UT, 84112, USA.
E-mail addresses: shuai.chen@jxstnu.edu.cn (S. Chen), marc.porter@utah.edu (M.D. Porter), lzang@eng.utah.edu (L. Zang).

https://doi.org/10.1016/j.aca.2023.340828
Received 7 September 2022; Received in revised form 21 December 2022; Accepted 11 January 2023
Available online 12 January 2023

donor-acceptor quenching of PDI by amines, which, when coupled with the concentrative nature of SPE, yields LODs for aniline and Kanamycin of 67 nM (~6 ppb) and 32 nM (~16 ppb), respectively.

1. Introduction

Driven by increases in the world's population and industrial manufacturing, the need for simple and easy-to-use tests for the analysis of contaminated water at the point of access continues to be a global imperative [1–3]. Today's most used approaches to water analysis include a range of hyphenated chromatographic-mass spectrometric techniques [4–8], electrochemistry [9–11], infrared (IR) and Raman spectrometry (including surface enhanced Raman scattering) [12–16], and other spectrometric methods [17]. However, the cost, footprint, power requirement and sample preparation processing often associated with these technologies limit their deployment beyond the formal laboratory setting. Electrochemical sensors, particularly those based on microfluidic [18] and 3D printed systems [19], hold great potential to address these technical limits regarding both form factor and portability, though the complications due to electrode surface modification and changes in background responses can impact repeatability and robustness when compared to spectrometry methods. In contrast, chemical sensors, like those based on fluorescence modulation have proven effective and robust in water quality monitoring by providing a simple, sensitive, and reliable means to detect a variety of organic and inorganic pollutants in water [1,20–24].

Like many other types of chemical sensors, quantitative detection with fluorescence sensors relies on stoichiometric interaction between fluorophore and analyte. As a result, these approaches require the ability to analyze an exacting volume of the sample. This requirement can complicate the practical use of fluorescence sensors, particularly in scenarios where quick, high throughput analysis may be a priority. Moreover, when the concentration of analyte in a sample is too low to produce a measurable fluorescence modulation, a preconcentration step is a necessity, which further magnifies the difficulty of onsite measurements. The development of approaches that eliminate the need for the analysis of a precise volume of sample would be an invaluable addition to field deployability.

This paper reports on a novel trace analysis technique, namely F-SPE, which couples fluorescent sensor with solid phase extraction (SPE) by modifying the SPE membrane with a fluorophore (Fig. 1), which, in this example, is a N,N′-di(nonyldecyl)-perylene-3,4,9,10-tetracarboxylic diimide or C9/9-PDI. When a water sample is passed through the SPE membrane, a certain amount of analyte will be absorbed, quenching the emission of the impregnated fluorophore. Herein, quantitative detection is based on the principle of negligible depletion (ND) intrinsic to SPE as applied to the extraction of analytes from solution [25–27]. With ND, the equilibrium amount of analyte extracted by the SPE membrane becomes dependent on the analyte concentration once the volume of solution flowing through the SPE membrane passes a threshold value. At this threshold volume, the extraction process has reached equilibrium and the concentration of sample existing in the membrane matches the concentration of sample entering into the membrane. This threshold volume is defined as the ND volume. Under the condition of ND, the amount of measured fluorescence quenching can be readily correlated with the analyte concentration by means of a calibration curve, which normally follows the Langmuir adsorption model. This allows for convenient onsite analysis simply by passing through a large enough volume of water sample without worrying about the need to precisely control the volume of sample analyzed. Moreover, depending on the porosity and surface area of the SPE substrate used, high levels of analyte preconcentration can be achieved, which enables lower levels of detection.

The concept of ND was previously applied by Porter et al. in the colorimetric detection of aqueous iodine, arsenite, dyes and other chemicals using SPE membranes [25,28–33], for which the amount of surface absorbed analytes was determined by diffuse reflectance spectrometry. One technical drawback of the method was that it could only be used for the detection of colored species or those with sufficient optical absorption in the UV–vis region. It is the aim of this study to expand the application of ND-SPE to the detection of essentially colorless analytes like amines by replacing colorimetric sensing with fluorescence sensing. In general, fluorescence sensing provides higher sensitivity than colorimetric sensing, thereby pushing the LOD to much lower levels.

In this study, we investigated the use of Empore™ SPE disks (a silica gel membrane modified with C18 groups) as a basis to access the merits of applying the ND-SPE to the fluorescence sensor (i.e., F-SPE) as described above (Fig. 1). The fluorophore used, C9/9-PDI, has the typical perylene diimide (PDI) molecular backbone structure. PDI molecules are highly fluorescent (quantum yield close to 100%) when dissolved in a solvent or immobilized on an inert surface, but can be quenched by photo-induced electron transfer (PET; Fig. 1), whereby PDI acts as an electron acceptor [34–37]. Using PDI as the fluorophore also takes advantage of the high thermal and photo-stabilities of the

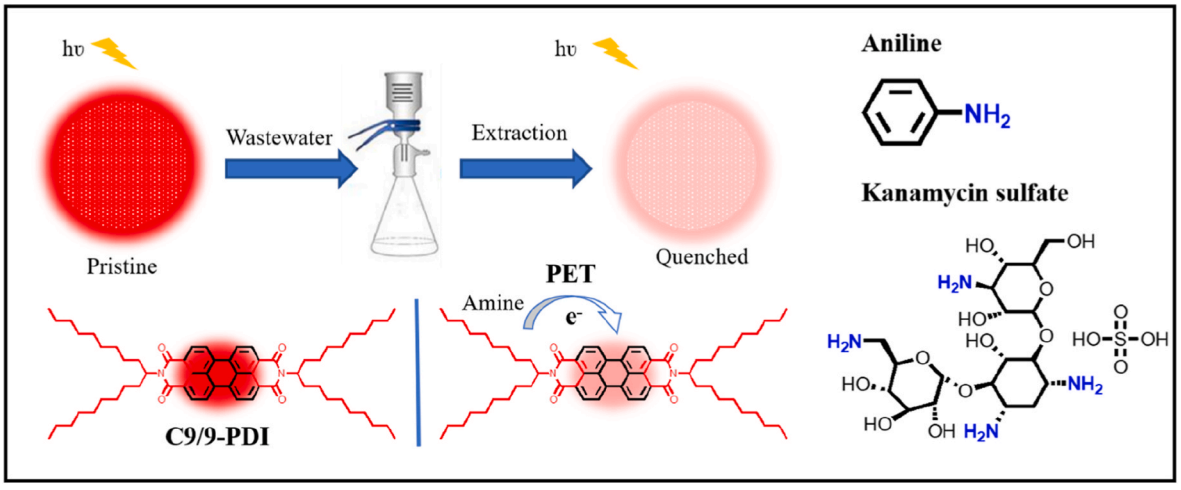

Fig. 1. Schematic of F-SPE by combining fluorescence sensing with SPE in a vacuum filtration setup. The sensing mechanism is based on fluorescence quenching via PET between amine and the fluorophore. Also, the molecular structure of C9/9-PDI used as the fluorophore, and aniline and Kanamycin (sulfate salt) are shown.

materials that have been extensively utilized in photovoltaics, light-emitting diodes, optoelectronics, and medical imaging and phototherapy [34–40].

For this study, we chose aniline and Kanamycin (an amine-containing antibiotic drug) (Fig. 1) as representative water pollutants. Organic amines usually function as strong electron donors and readily quench the fluorescence of PDIs through photoinduced electron transfer [34,41–43]. It is thus expected that the presence of amines in water can be detected by the SPE disk coated with PDI via fluorescence quenching. Moreover, amine-containing compounds constitute an important class of water pollutants which can be detrimental to the ecological environment, biological health and economic security [44–46]. Aniline, for example, is highly poisonous to human and animals and can cause serious health and environment threats when is discharged into water systems. Aniline can also cause detrimental effects to the microorganisms used in the water treatment processes. Many drugs such as antibiotics also have multiple amine groups in their large molecular structure, and can be classified as amine-containing compounds. When present in water, these drugs may cause even greater problems to the aquatic ecosystems than the normal amines due to the medical effects on humans and other living species [47,48]. Therefore, it is of significant interest to develop simple methods for quick onsite detection of these pollutants. High throughput monitoring of drugs, particularly antibiotics, in various locations helps create dynamic mapping of the pollution in water systems including rivers and lakes, which is especially crucial for the countries where antibiotics are widely used.

2. Experimental section

2.1. Reagents and chemicals

n-Propanol, Kanamycin ($C_{18}H_{36}N_4O_{11}$, MW: 484.5 g/mol), and its sulfate salt, and acetic acid were purchased from Aladdin Reagent Co., Ltd (China). Aniline, NaCl, NaOH, Na_2SO_4, KH_2PO_4 were acquired from Macklin reagent Co., Ltd (China). All chemicals and reagents were of analytical grade quality, and used without further purification. Deionized (DI) water was prepared with a EPED-Smart-S2 water purification system (Nanjing Yipu Yida Technology Development Co., China). C9/9-PDI was synthesized and purified following a protocol previously developed in our laboratory [49]. Molecularly dispersed (i.e., non-aggregated) stock solutions (100 μM) of C9/9-PDI was prepared in n-propanol. Stock solutions of aniline (10 mM) and Kanamycin (100 μM), and all the spiked samples used in the test were prepared with DI water.

2.2. Fabrication of fluorophore modified SPE disks

The fluorescent SPE disks were prepared by coating Empore™ SPE disks with C9/9-PDI. Empore™ disk consists of C18-modified silica particles (~12 μm diameter) enmeshed in fibril-based polytetrafluoroethylene (PTFE) membranes (0.5 mm thickness) at 90% silica:10% PTFE (w/w). Surface coatings were prepared by passing 10 mL of C9/9-PDI solution (10 μM in n-propanol) through the disk by using the vacuum filtration setup (Fig. S1) at a flow rate of 0.08 mL/min for a total time of ~12 min; a few higher flow rates were tested, e.g., 0.7 and 1 mL/min, but yielded visually heterogeneous precipitates on the outer surface of the membrane. The hydrophobic nature and chain structure of the C18-modified silica particles strongly adsorb the fluorophore by interdigitating with the C9 side chains of C9/9-PDI, dispersing it across the silica surface with little observable aggregation (*vide infra*). A few other C9/9-PDI concentrations and flow rates were tested, but the above condition resulted in the most homogeneous distribution of the fluorophore across the membrane by visual inspection.

2.3. Instrumentation, optical measurements, and data analysis

The UV–vis absorption spectra of C9/9-PDI in n-propanol were measured using a Shimadzu spectrophotometer (UV-2600). The fluorescence spectra of the samples were acquired with an Edinburgh fluorometer (model FS5). A fluorescence microscope (OST-YW4000, Suzhou Oust Optical Instrument Co., Ltd.; China), set at a magnification of 400 × (2 mm cylindrical spot size) was used to obtain fluorescence images of the samples.

When used in F-SPE (Fig. 1), the fluorescence of the C9/9-PDI coated disk changes upon pulling aqueous amine-containing solutions through it by vacuum filtration. The changes in emission were measured using a field-portable fluorometer (USB4000-FL, Ocean Optics), which was equipped with a flexible optical fiber probe for optical excitation delivery and emission collection (Fig. S2). The angle of incidence for the optical fiber bundle was set at 45° with respect to the SPE disk surface. The excitation beam had a diameter of 2 mm. The data collected by the fiber optic spectrometer were uploaded to a spreadsheet on a computer for calculation of relative fluorescence intensities, construction of calibration and Langmuir isotherm plots, and estimation of LOD.

3. Results and discussion

3.1. F-SPE disk preparation and spectral characteristics

Spectra demonstrating the successful and reproducible impregnation of the fluorophore in the SPE disk and the stability of impregnation in wash-off tests are given in Fig. 2 and S3. Fig. 2A is the spectrum for C9/9-PDI dissolved in neat n-propanol (10 μM), which shows three distinct emission maxima (540, 578, and 630 nm), corresponding to the 0 → 0, 0 → 1 and 0 → 2 transitions, respectively. This spectral profile, which includes the relative differences in the strength of the three bands, is a signature for C9/9-PDI when it is molecularly dispersed (i.e., non-aggregated) in a solvent like n-propanol [49,50].

Fig. 2B presents fluorescence spectra for the SPE disk impregnated with C9/9-PDI measured after each rinse for a total of eight consecutive rinses (10 mL of DI water per rinse) using vacuum filtration. There are three points to draw from these spectra. First, the spectral profile for the impregnated fluorophore (emission maxima at 536, 578, and 626 nm) closely matches that for C9/9-PDI when dissolved in n-propanol. This confirms the ability to load the disk with C9/9-PDI. Second, the strong similarities of the spectral profiles of the spectra for the solution and immobilized fluorophore indicate that the impregnated C9/9-PDI is well dispersed in a molecular state [49]. This assessment is consistent with the visual uniformity of the green fluorescence intensity across the SPE disk shown in the inset to Fig. 2B. The molecular dispersion of impregnated C9/9-PDI is attributed to the strong intermolecular association/interdigitation of the C9 chains of C9/9-PDI and the C18 chains coated on the silica particles of the Empore™ disk [51–53]. There is no detectable evidence for aggregated fluorophore, which otherwise has a single emission maximum at ~620 nm across the same spectral region [49]. Third, the fluorescence spectra measured for the same disk across eight separate water washes shows a high level of consistency. This consistency documents the stability of immobilized C9/9-PDI when rinsed with water. The stability against water is also ascribed to the strong surface association of C9/9-PDI as mentioned above. Moreover, C9/9-PDI is insoluble in water, also making it difficult to be washed away by water. The small fluctuations of fluorescence intensity shown in Fig. 2B is likely due to the rough surface of the disk, which may cause certain level of fluctuation for the emission measurement, especially via an optic fiber. In view of the observed measurement fluctuations, the averaged fluorescence intensity from 5 measurements at the same position on the substrate was used in all subsequent analysises.

The impregnation of C9/9-PDI was also proven reproducible as shown in Fig. S3. The fluorescence spectra measured for the five separately modified disks demonstrate a high level of consistency, e.g., the

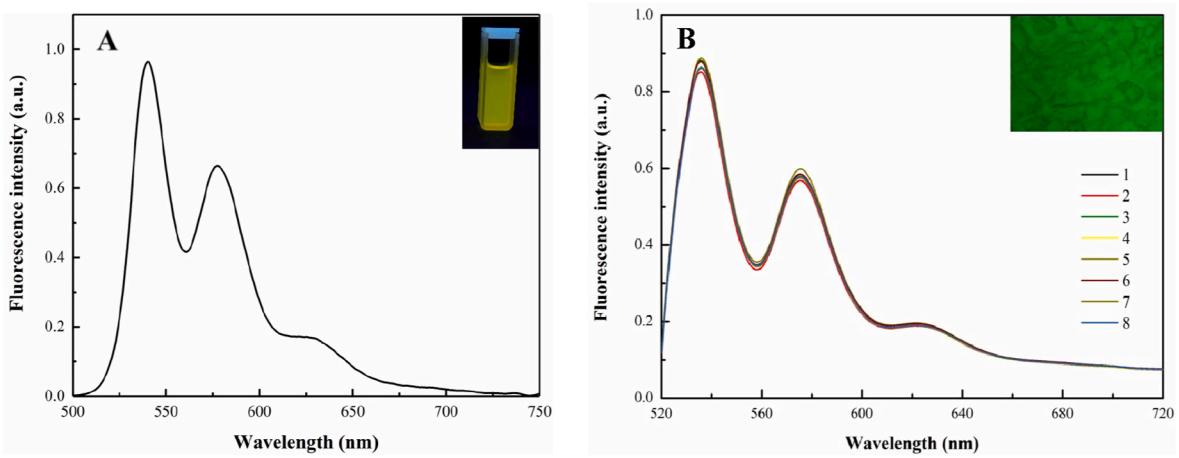

Fig. 2. (A) Fluorescence spectra measured for a 10 μM solution of C9/9-PDI in n-propanol (λ_{ex}: 490 nm). The inset shows the fluorescence photograph of the solution in a quartz cuvette. (B) Fluorescence spectra recorded for an Empore™ disk coated with C9/9-PDI for each of eight consecutive rinses with 10 mL of deionized water (via vacuum filtration). The inset shows the fluorescence microscopy image (400 ×) of the disk.

emission intensities of the 536 nm band for the five samples differ by only ~4%. This low variability confirms the reproducibility of impregnation. The high reproducibility is attributed to the intrinsic homogeneous matrix of Empore™ disk and the effectiveness of the impregnation process facilitated by the strong surface association of C9/9-PDI. Highly repeatable fabrication of sensor materials is critical for translating a sensor technique to practical applications.

3.2. F-SPE and ND

3.2.1. Sampling volume as defined by the principle of ND

The results from measurements to determine the ND volume for aniline at two different aqueous solution concentrations (1 and 10 μM) with C9/9-PDI modified SPE disks are presented in Fig. 3. Sample volumes from 0 to 60 mL (10 mL increments) were tested. As is apparent, the fluorescence intensities for both aniline concentrations decrease as the volume of sample passed through the disk increases, reach limiting values at ~40 mL, and remain effectively unchanged at larger sample volumes. These results indicate a ND volume of 40 mL for this combination of analyte and fluorophore-modified disk. The change in signal with volume of solution passed through the impregnated membrane also shows that the amount of fluorescence quenching for the 10 μM aniline solution is greater than that for the 1 μM solution. Both observations follow expectations for a well-behaved system operating under the condition of ND, i.e., the fluorescence quenching of the disk can be correlated with the equilibrium concentration of solution as defined by the Langmuir adsorption model and static quenching mechanism (*vide infra*).

The same procedure was used to establish the ND volume for the analysis of Kanamycin (1 and 10 μM aqueous solutions) using the same SPE disk modified with C9/9-PDI. These results are presented in Fig. 4. Like the dependence found for aniline (Fig. 3), the strength of the fluorescence decreases with the volume of sample passed through the disk. In the case of Kanamycin, however, the responses plateau at a sample volume of ~20 mL, which is roughly half that required for aniline. The smaller value of ND volume found for Kanamycin is attributed to the stronger intermolecular interaction with C9/9-PDI, for which the binding constant is about 2.5 times higher than that for aniline as deduced from the fluorescence quenching data (*vide infra*). The stronger affinity allows Kanamycin to reach the equilibration (as probed by the

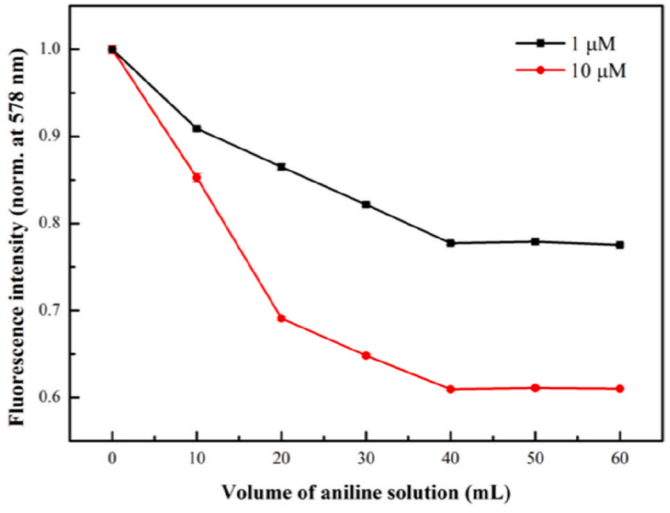

Fig. 3. Fluorescence intensity measured for the C9/9-PDI coated Empore™ disk after filtering with varying volumes of water solutions of aniline under vacuum, for which two series of experiments were performed with two different concentrations of aniline, 1 and 10 μM.

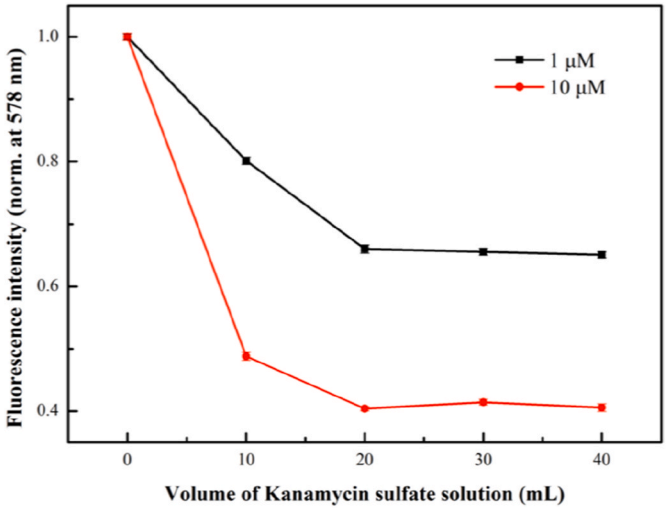

Fig. 4. Fluorescence intensity measured for the C9/9-PDI coated Empore™ disk after filtering with varying volumes of water solutions of Kanamycin under vacuum, for which two series of experiments were performed with two different concentrations of Kanamycin, 1 and 10 μM.

fluorescence quenching) more effectively at lower ND volumes.

3.2.2. Binding equilibrium and LOD

When the volume of a sample passing through the SPE disk is at or above ND value, the uptake of analyte by the disk is at equilibrium, and the surface concentration of analyte (C_s) can be correlated with the solution concentration (C) following the classic Langmuir adsorption model [54], [[,55].

$$C_s = \frac{C_s^0 KC}{1 + KC} \tag{1}$$

where C_s^o is the maximum surface concentration of analytes when all the adsorption sites are occupied, and K is the adsorption equilibrium constant. For a given SPE disk, C_s^o is a constant.

The surface adsorbed analytes will interact with the fluorophore embedded in the SPE disk, resulting in fluorescence quenching, which can be described as a typical static process in the format of Stern-Volmer equation [56].

$$\frac{I_0}{I} = 1 + K' C_s \tag{2}$$

where I_0 is the fluorescence intensity measured in the absence of analytes, I is the intensity at a given surface concentration of analytes, and K' is the binding constant between the analyte and fluorophore.

Combining Eqs. (1) and (2) gives

$$\frac{I_0 - I}{I_0} = \frac{C_s^0 K' KC}{1 + \left(1 + C_s^0 K'\right) KC} \tag{3}$$

Eq. (3) correlates the fluorescence quenching efficiency, defined as of $(I_0–I)/I_0$, directly with the concentration of analytes, thus enabling quantitative detection of analytes simply by measuring the fluorescence intensity change.

Fig. 5 presents the results and analysis of data from measuring the fluorescence of C9/9-PDI impregnated disks as a function of aniline concentration. Fig. 5A shows the expected decrease in fluorescence as the concentration of aniline increases. These spectra were used to generate the plot of $(I_0–I)/I_0$ as a function of aniline concentration presented in Fig. 5B, for which the fluorescence quenching data obtained can be fitted very well with Eq. (3) (with a R^2 value of 0.998), producing values of K ($3.7 \pm 0.5 \times 10^5$ M^{-1}) and C_s^oK' (0.83 ± 0.04) for aniline. The fit can be used as a calibration curve to estimate the LOD, which is defined as the concentration of sample that corresponds to the blank signal plus three times its standard deviation [57–59]. Accordingly, the LOD for aniline is projected to be 67 nM (~6 ppb). The LOD thus obtained is lower than most of the values reported recently for many other fluorescence sensors, such as those based on metal-organic-framework (MOF) [60–62], hydrogen-bonded organic framework [63], and modified BODIPY fluorophores [64]. Even lower LOD (3 nM) was reported on a fluorescence turn-on sensor based on 2D coordination network constructed from hexacopper(I)-iodide clusters and cage-like aminophosphine blocks [65]. However, the construction of this type of sensor materials requires an often tedious series of molecular and polymeric syntheses and intricate structural engineering. Summary comparisons of these sensors with our F-SPE sensor regarding LOD and other performance metrics can be found in Table S1. To further test the adaptability of F-SPE for analysis of real water samples, the same experiments shown in Fig. 5 were repeated for the samples prepared in tap water. The results obtained (Fig. S4) demonstrate a strong consistency with respect to with Fig. 5 in terms of both fluorescence quenching measurement and fitting of data with Langmuir adsorption model (Eq. (3)), implying that the detection of amine with F-SPE is not significantly affected by the interferents like inorganic ions commonly present in tap water.

In completing our concept assessment of F-SPE, we tested its extensibility by analyzing water samples spiked with Kanamycin. The results of these experiments are shown by the spectral data in Fig. 6A and fluorescence quenching dependence as a function of Kanamycin concentration in Fig. 6B. As observed for aniline, the fluorescence quenching data obtained for Kanamycin shown in Fig. 6B can also be fitted very well with Eq. (3) (with a R^2 value of 0.999), producing values of K ($2.9 \pm 0.3 \times 10^5$ M^{-1}) and C_s^oK' (2.09 ± 0.06) for Kanamycin. The value of K obtained for Kanamycin is slightly lower than that for aniline, which is consistent with its slightly higher hydrophobicity of aniline, as implied from the solubility of aniline and Kanamycin in water, 35 and 50 g/L [66,67]. Since Empore™ disk is composed of C18-modifed silica gel embedded in PTFE matrix, the surface adsorption would be more preferred for hydrophobic molecule. The value of K' obtained for Kanamycin is about 2.5 times larger than that for aniline, indicating the stronger electron donor-acceptor binding interaction between Kanamycin and C9/9-PDI, which is in turn consistent with the fact that there are four amine groups (acting as the electron donor) contained in Kanamycin, while there is only one amine group in aniline.

Using the fitting data from Fig. 6B, we can estimate a LOD of 32 nM for Kanamycin. This level obtained is comparable to or even better than that achieved with the sophisticated detection technologies developed previously for Kanamycin, such as those based on surface plasmon resonance (SPR) spectroscopy [68], liquid chromatography coupled

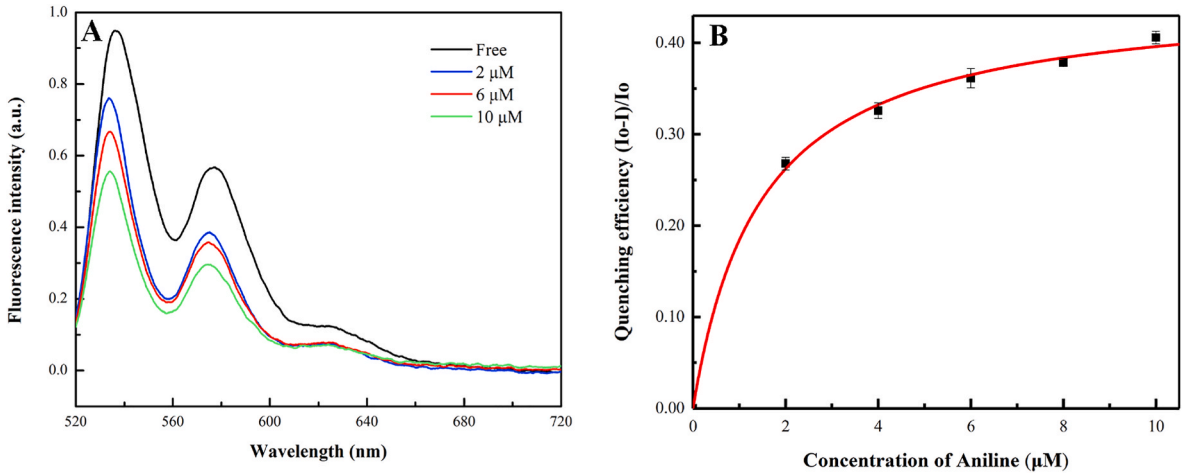

Fig. 5. (A) Fluorescence spectra of the Empore™ disk coated with C9/9-PDI measured before and after passage of 60 mL of aniline solution of varying concentrations. (B) The corresponding fluorescence quenching efficiency was plotted as a function of the concentration of aniline, and all the data points can be fitted well with Eq. (3). The sample volume used, 60 mL, is above the ND volume (40 mL) determined for aniline with the Empore™ disk (Fig. 3).

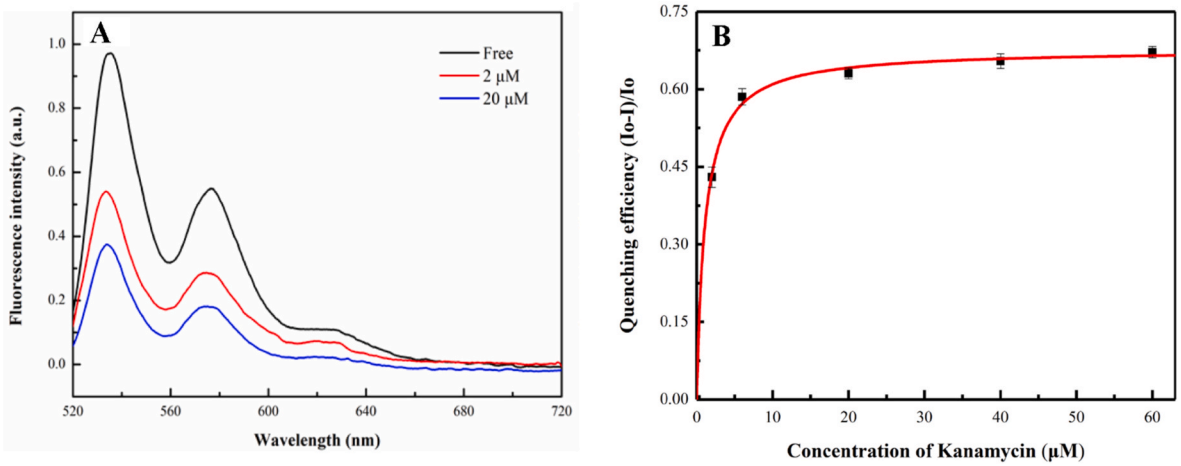

Fig. 6. (A) Fluorescence spectra of an Empore™ disk (C) coated with C9/9-PDI measured before and after passing through 40 mL of Kanamycin solution of varying concentrations. (B) The corresponding fluorescence quenching efficiency was plotted as a function of the concentration of Kanamycin, and all the data points can be fitted well with Eq. (3). The sample volume used, 40 mL, is above the ND volume (20 mL) determined for Kanamycin with the with the Empore™ disk (Fig. 4).

with pulsed electrochemical detection [69], liquid chromatography combined with SPE and tandem mass spectrometry [70]. While even lower LODs (<10 nM) were reported for some other sensor systems, most of the sensors are either challenging for operation and control, or involve complicated material synthesis and engineering [71–73], thus not suited for immediate deployment in practical applications. To this regard, the F-SPE technique developed herein may find an easy practical path in the detection or screening of antibiotics and other drugs in water environments, taking combined advantages of the low LOD and simple process intrinsic of the ND concept of SPE. It is interesting to see from Figs. 5 and 6 that the extraction of both aniline and Kanamycin reaches saturation in fluorescence quenching as the concentration increases, and the saturated value is apparently dependent on the analytes. This can be interpreted as a limited condition of Eq. (3). When the solution concentration C increases to be sufficiently high, i.e., $KC \gg 1$, Eq. (3) can be approximated as Eq. (4),

$$\frac{I_0 - I}{I_0} = \frac{C_s^0 K'}{C_s^0 K' + 1} \tag{4}$$

which implies that the fluorescence quenching efficiency will become saturated, reaching a plateau with the value determined only by the two constants, C_s^o and K', when the concentration of analytes increases. Apparently, for a given SPE disk (with C_s^o fixed) the saturated quenching efficiency would depend solely on the intermolecular binding constant K'.

3.2.3. *Fluorescent sensing selectivity towards amines*

As discussed above, C9/9-PDI is a typical electron acceptor, and the fluorescence quenching is usually a result of interaction with an electron donor like aniline or other amines. In the water environment under ambient conditions, there are few molecules or ions that can compete effectively with amines functioning as an electron donor to enable fluorescence quenching of PDI. It is thus expected that the PDI sensor should demonstrate high selectivity towards amines vs. other common chemicals present in water environment such as alcohols, aldehydes, acetone, phenols, nitroaromatics, alkanes, surfactants, acetic acid, metal ions, anions, which can be considered as potential interferents to the F-SPE detection. To test such sensing selectivity, we performed the fluorescence quenching of PDI in ethanol solution by five different amines (aniline, benzylamine, phenethylamine, cyclohexylamine and butylamine) in comparison to 16 common interferents in water under the same condition (Fig. 7). All the five amines showed significant quenching, though the quenching efficiency of aniline was found about 4 × times higher than that of the other four amines, which is mainly due

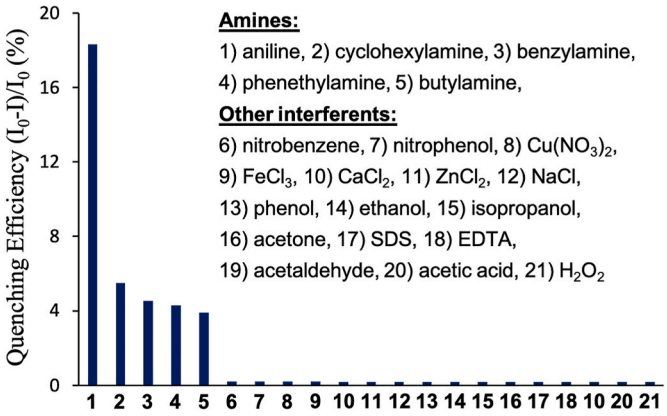

Fig. 7. Fluorescence quenching efficiency of C9/9-PDI fluorophore measured in ethanol solution (2 μM) for 5 amines in comparison to 16 other chemicals commonly found in environmental water samples. All of the chemicals were tested under the same concentration (5 mM).

to the aromatic nature of aniline that increases its strength as an electron donor. In contrast to the amines, all of the 16 interferents exhibit a minimal signal response (with quenching efficiency at or below 0.25%) when tested at the same concentration. This indicates a high level of selectivity by the PDI fluorophore towards amines as a class of analytes. Nonetheless, it is not possible for a single fluorophore to discriminate amines among a broad range of analogues due to their close structure and chemical properties. In general, a more realistic approach to achieving detection specificity would be incorporating different fluorophores onto a F-SPE disk patterned as an array, which will enable differential sensing. By coupling with automated machine learning, the differential sensing based on an array can usually provide high level discrimination power, even for the chemical analogues with very similar structure or properties, as evidenced in many other studies [74–77].

4. Conclusions

We have developed a new SPE-based detection technology, namely F-SPE, by combining fluorescent sensor with solid phase extraction (SPE). The F-SPE technology developed can detect trace level of aniline and Kanamycin in water, with LOD down to 67 nM and 32 nM, respectively. The LODs obtained compare favorably to those reported for the fluorescence sensors based on different materials and sensing

mechanisms. The main innovation of this work and the associated impact to chemical and biochemical analysis lie in coupling the intrinsic high sensitivity of fluorescent sensors to two unique features of SPE, i.e., the strong concentrative nature of SPE (usually with a concentrative factor of >1000) and the principle of negligible depletion (ND) that significantly simply the analysis process by eliminating the need to precisely control the volume of sample analyzed. Combining the high sensitivity, simplicity of use, and low cost, the F-SPE technology has great potential to be applied in detection of broad range of water pollutants by taking advantage of the extensibility of the design of fluorophores to target different types of chemicals.

CRediT authorship contribution statement

Miao Zhang: Formal analysis. **Rana Dalapati:** Formal analysis. **Jiangfan Shi:** Formal analysis. **Chenglong Liao:** Formal analysis. **Qingyun Tian:** Formal analysis. **Xiaomei Yang:** Formal analysis. **Shuai Chen:** Supervision. **Marc D. Porter:** Supervision. **Ling Zang:** Supervision.

Declaration of competing interest

The authors declare that they have no known competing financial interests or personal relationships that could have appeared to influence the work reported in this paper.

Data availability

Data will be made available on request.

Acknowledgements

This work was supported by the financial support from the Scientific Research Fund of Shaanxi University of Science and Technology and University of Utah. We would also like to dedicate this work to our colleague James S. Fritz to invaluable discussions about SPE over the past several years.

Appendix A. Supplementary data

Supplementary data to this article can be found online at https://doi.org/10.1016/j.aca.2023.340828.

References

[1] H. Sohrabi, A. Hemmati, M.R. Majidi, S. Eyvazi, A. Jahanban-Esfahlan, B. Baradaran, R. Adlpour-Azar, A. Mokhtarzadeh, M. de la Guardia, Recent advances on portable sensing and biosensing assays applied for detection of main chemical and biological pollutant agents in water samples: a critical review, TrAC, Trends Anal. Chem. 143 (2021), 116344.
[2] T. Rasheed, M. Bilal, F. Nabeel, M. Adeel, H.M.N. Iqbal, Environmentally-related contaminants of high concern: potential sources and analytical modalities for detection, quantification, and treatment, Environ. Int. 122 (2019) 52–66.
[3] Y. Tang, M. Yin, W. Yang, H. Li, Y. Zhong, L. Mo, Y. Liang, X. Ma, X. Sun, Emerging pollutants in water environment: occurrence, monitoring, fate, and risk assessment, Water Environ. Res. 91 (10) (2019) 984–991.
[4] V. Castro, J.B. Quintana, I. Carpinteiro, J. Cobas, N. Carro, R. Cela, R. Rodil, Combination of different chromatographic and sampling modes for high-resolution mass spectrometric screening of organic microcontaminants in water, Anal. Bioanal. Chem. 413 (22) (2021) 5607–5618.
[5] Y. Du, X. Xu, Q. Liu, L. Bai, K. Hang, D. Wang, Identification of organic pollutants with potential ecological and health risks in aquatic environments: progress and challenges, Sci. Total Environ. 806 (2022), 150691.
[6] J. da Silva Sousa, H.O. do Nascimento, H. de Oliveira Gomes, R.F. do Nascimento, Pesticide residues in groundwater and surface water: recent advances in solid-phase extraction and solid-phase microextraction sample preparation methods for multiclass analysis by gas chromatography-mass spectrometry, Microchem. J. 168 (2021), 106359.
[7] J.F. Ayala-Cabrera, F.J. Santos, E. Moyano, Recent advances in analytical methodologies based on mass spectrometry for the environmental analysis of halogenated organic contaminants, Trends Environ. Analyt. Chem. 30 (2021), e00122.
[8] T. Reemtsma, Liquid chromatography–mass spectrometry and strategies for trace-level analysis of polar organic pollutants, J. Chromatogr. A 1000 (1) (2003) 477–501.
[9] Y. Liu, Q. Xue, C. Chang, R. Wang, Z. Liu, L. He, Recent progress regarding electrochemical sensors for the detection of typical pollutants in water environments, Anal. Sci. 38 (1) (2022) 55–70.
[10] G. Hanrahan, D.G. Patil, J. Wang, Electrochemical sensors for environmental monitoring: design, development and applications, J. Environ. Monit. 6 (8) (2004) 657–664.
[11] Q. Tian, S. Chen, J. Yu, M. Zhang, N. Gao, X. Yang, C. Wang, X. Duan, L. Zang, Tunable construction of electrochemical sensors for chlorophenol detection, J. Mater. Chem. C 10 (28) (2022) 10171–10195.
[12] S. Veerasingam, M. Ranjani, R. Venkatachalapathy, A. Bagaev, V. Mukhanov, D. Litvinyuk, M. Mugilarasan, K. Gurumoorthi, L. Guganathan, V.M. Aboobacker, P. Vethamony, Contributions of Fourier transform infrared spectroscopy in microplastic pollution research: a review, Crit. Rev. Environ. Sci. Technol. 51 (22) (2021) 2681–2743.
[13] T. Dey, Microplastic pollutant detection by surface enhanced Raman spectroscopy (SERS): a mini-review, Nanotechnol. Environ.Eng. (2022), https://doi.org/10.1007/s41204-022-00223-7.
[14] R. Moldovan, B.-C. Iacob, C. Farcău, E. Bodoki, R. Oprean, Strategies for SERS Detection of Organochlorine Pesticides *Nanomaterials* [Online], 2021.
[15] V. Brahmkhatri, P. Pandit, P. Rananaware, A. D'Souza, M.D. Kurkuri, Recent progress in detection of chemical and biological toxins in Water using plasmonic nanosensors, Trends Environ. Analyt. Chem. 30 (2021), e00117.
[16] G. Bodelón, I. Pastoriza-Santos, Recent progress in surface-enhanced Raman scattering for the detection of chemical contaminants in water, Front. Chem. 8 (2020).
[17] B.S. Rathi, P.S. Kumar, D.-V.N. Vo, Critical review on hazardous pollutants in water environment: occurrence, monitoring, fate, removal technologies and risk assessment, Sci. Total Environ. 797 (2021), 149134.
[18] Sunaina, H. Kaur, N. Kumari, A. Sharma, M. Sachdeva, V. Mutreja, Optical and electrochemical microfluidic sensors for water contaminants: a short review, Mater. Today Proc. 48 (2022) 1673–1679.
[19] J. Muñoz, M. Pumera, Accounts in 3D-printed electrochemical sensors: towards monitoring of environmental pollutants, Chemelectrochem 7 (16) (2020) 3404–3413.
[20] S. Chen, Z. Xue, N. Gao, X. Yang, L. Zang, Perylene diimide-based fluorescent and colorimetric sensors for environmental detection, Sensors 20 (3) (2020).
[21] L. Walekar, T. Dutta, P. Kumar, Y.S. Ok, S. Pawar, A. Deep, K.-H. Kim, Functionalized fluorescent nanomaterials for sensing pollutants in the environment: a critical review, TrAC, Trends Anal. Chem. 97 (2017) 458–467.
[22] G.A. Ibañez, G.M. Escandar, Luminescence sensors applied to water analysis of organic pollutants—an update, Sensors 11 (12) (2011).
[23] M.I. Gaviria-Arroyave, J.B. Cano, G.A. Peñuela, Nanomaterial-based fluorescent biosensors for monitoring environmental pollutants: a critical review, Talanta Open 2 (2020), 100006.
[24] Y.-H. Shin, M. Teresa Gutierrez-Wing, J.-W. Choi, Review—recent progress in portable fluorescence sensors, J. Electrochem. Soc. 168 (1) (2021), 017502.
[25] N.C. Dias, M.D. Porter, J.S. Fritz, Principles and applications of colorimetric solid-phase extraction with negligible depletion, Anal. Chim. Acta 558 (1) (2006) 230–236.
[26] J. Pawliszyn, Theory of solid-phase microextraction, J. Chromatogr. Sci. 38 (7) (2000) 270–278.
[27] L. Nardi, Capillary extractors for "negligible depletion" sampling of benzene, toluene, ethylbenzene and xylenes by in-tube solid-phase microextraction, J. Chromatogr. A 985 (1) (2003) 85–91.
[28] M.M. Bradley, L.M. Siperko, M.D. Porter, Colorimetric-solid phase extraction method for trace level determination of arsenite in water, Talanta 86 (2011) 64–70.
[29] D.B. Gazda, J.R. Schultz, L.M. Siperko, M.D. Porter, R.J. Lipert, S.M. Flint, J. T. McCoy, In In-Flight Water Quality Monitoring On the International Space Station (ISS): Measuring Biocide Concentrations With Colorimetric Solid Phase Extraction (CSPE), 40th International Conference on Environmental Systems, 2010. Barcelona; Spain, 11-15 Jul. 2010; Barcelona; Spain.
[30] D. Gazda, R. Lipert, J. Fritz, M. Porter, Rapid determination of biocide concentrations using colorimetric solid phase extraction (C-SPE): results from microgravity testing, SAE Technical Paper (2003), https://doi.org/10.4271/2003-01-2406, 2003-01-2406.
[31] D.B. Gazda, R.J. Lipert, J.S. Fritz, M.D. Porter, Investigation of the iodine–poly (vinylpyrrolidone) interaction employed in the determination of biocidal iodine by colorimetric solid-phase extraction, Anal. Chim. Acta 510 (2) (2004) 241–247.
[32] A.A. Hill, R.J. Lipert, J.S. Fritz, M.D. Porter, A rapid, simple method for determining formaldehyde in drinking water using colorimetric-solid phase extraction, Talanta 77 (4) (2009) 1405–1408.
[33] A.A. Hill, R.J. Lipert, M.D. Porter, Determination of colloidal and dissolved silver in water samples using colorimetric solid-phase extraction, Talanta 80 (5) (2010) 1606–1610.
[34] M. Zhang, J. Shi, C. Liao, Q. Tian, C. Wang, S. Chen, L. Zang, Perylene imide-based optical chemosensors for vapor detection, Chemosensors 9 (1) (2021) 1.
[35] L. Zang, Interfacial donor–acceptor engineering of nanofiber materials to achieve photoconductivity and applications, Accounts Chem. Res. 48 (10) (2015) 2705–2714.
[36] S. Chen, P. Slattum, C. Wang, L. Zang, Self-Assembly of perylene imide molecules into 1D nanostructures: methods, morphologies, and applications, Chem. Rev. 115 (21) (2015) 11967–11998.

[37] L. Zang, Y. Che, J.S. Moore, One-dimensional self-assembly of planar π-conjugated molecules: adaptable building blocks for organic nanodevices, Accounts Chem. Res. 41 (12) (2008) 1596–1608.
[38] S. Chen, N. Gao, B.R. Bunes, L. Zang, Tunable nanofibril heterojunctions for controlling interfacial charge transfer in chemiresistive gas sensors, J. Mater. Chem. C 7 (44) (2019) 13709–13735.
[39] D. McDowall, B.J. Greeves, R. Clowes, K. McAulay, A.M. Fuentes-Caparrós, L. Thomson, N. Khunti, N. Cowieson, M.C. Nolan, M. Wallace, A.I. Cooper, E. R. Draper, A.J. Cowan, D.J. Adams, Controlling photocatalytic activity by self-assembly – tuning perylene bisimide photocatalysts for the hydrogen evolution reaction, Adv. Energy Mater. (2020), 2002469 n/a (n/a).
[40] Z. Yang, X. Chen, Semiconducting perylene diimide nanostructure: multifunctional phototheranostic nanoplatform, Accounts Chem. Res. 52 (5) (2019) 1245–1254.
[41] Y. Che, X. Yang, S. Loser, L. Zang, Expedient vapor probing of organic amines using fluorescent nanofibers fabricated from an n-type organic semiconductor, Nano Lett. (2008) 2219–2223.
[42] Y. Che, L. Zang, Enhanced fluorescence sensing of amine vapor based on ultrathin nanofibers, Chem. Commun. (2009) 5106–5108.
[43] N. Wu, C. Wang, B.R. Bunes, Y. Zhang, P.M. Slattum, X. Yang, L. Zang, Chemical self-doping of organic nanoribbons for high conductivity and potential application as chemiresistive sensor, ACS Appl. Mater. Interfaces 8 (19) (2016) 12360–12368.
[44] L. Wang, X. Ran, H. Tang, D. Cao, Recent advances on reaction-based amine fluorescent probes, Dyes Pigments 194 (2021), 109634.
[45] P. Campo, W. Platten, M.T. Suidan, Y. Chai, J.W. Davis, Aerobic biodegradation of amines in industrial saline wastewaters, Chemosphere 85 (7) (2011) 1199–1203.
[46] N.A. Khan, A.H. Khan, P. Tiwari, M. Zubair, M. Naushad, New insights into the integrated application of Fenton-based oxidation processes for the treatment of pharmaceutical wastewater, J. Water Proc. Eng. 44 (2021), 102440.
[47] C. Fu, B. Xu, H. Chen, X. Zhao, G. Li, Y. Zheng, W. Qiu, C. Zheng, L. Duan, W. Wang, Occurrence and distribution of antibiotics in groundwater, surface water, and sediment in Xiong'an New Area, China, and their relationship with antibiotic resistance genes, Sci. Total Environ. 807 (2022), 151011.
[48] N. Ma, L. Tong, Y. Li, C. Yang, Q. Tan, J. He, Distribution of antibiotics in lake water-groundwater - sediment system in Chenhu Lake area, Environ. Res. 204 (2022), 112343.
[49] K. Balakrishnan, A. Datar, T. Naddo, J. Huang, R. Oitker, M. Yen, J. Zhao, L. Zang, Effect of side-chain substituents on self-assembly of perylene diimide molecules: morphology control, J. Am. Chem. Soc. 128 (2006) 7390–7398.
[50] X. Du, J. Zhou, J. Shi, B. Xu, Supramolecular hydrogelators and hydrogels: from soft matter to molecular biomaterials, Chem. Rev. 115 (24) (2015) 13165–13307.
[51] Y. Che, H. Huang, M. Xu, C. Zhang, B.R. Bunes, X. Yang, L. Zang, Interfacial engineering of organic nanofibril heterojunctions into highly photoconductive materials, J. Am. Chem. Soc. 133 (2011) 1087–1091.
[52] C. Wang, B.R. Bunes, M. Xu, N. Wu, X. Yang, D.E. Gross, L. Zang, Interfacial donor–acceptor nanofibril composites for selective alkane vapor detection, ACS Sens. 1 (5) (2016) 552–559.
[53] C.E. McCold, Q. Fu, S. Hihath, J.-M. Han, Y. Halfon, R. Faller, K. van Benthem, L. Zang, J. Hihath, Ligand exchange based molecular doping in 2D hybrid molecule-nanoparticle arrays: length determines exchange efficiency and conductance, Molecular Sys. Design Eng. 2 (4) (2017) 440–448.
[54] P.S. Ghosal, A.K. Gupta, Development of a generalized adsorption isotherm model at solid-liquid interface: a novel approach, J. Mol. Liq. 240 (2017) 21–24.
[55] S. Azizian, S. Eris, L.D. Wilson, Re-evaluation of the century-old Langmuir isotherm for modeling adsorption phenomena in solution, Chem. Phys. 513 (2018) 99–104.
[56] J.R. Lakowicz, Principles of Fluorescence Spectroscopy, second ed., Plenum Publishers, New York, NY, 1999.
[57] C. Liao, M. Zhang, N. Gao, Q. Tian, J. Shi, S. Chen, C. Wang, L. Zang, Paper-based vapor detection of formaldehyde: colorimetric sensing with high sensitivity, Chemosensors 9 (12) (2021) 335.
[58] M. Xu, J.M. Han, Y. Zhang, X. Yang, L. Zang, Selective fluorescence turn-on sensor for trace vapor detection of hydrogen peroxide, Chem. Commun. 49 (100) (2013) 11779–11781.
[59] M. Xu, B.R. Bunes, L. Zang, Paper-based vapor detection of hydrogen peroxide: colorimetric sensing with tunable interface, ACS Appl. Mater. Interfaces 3 (2011) 642–647.
[60] J.-Y. Zou, L. Li, S.-Y. You, H.-M. Cui, Y.-W. Liu, K.-H. Chen, Y.-H. Chen, J.-Z. Cui, S.-W. Zhang, Sensitive luminescent probes of aniline, benzaldehyde and Cr(VI) based on a zinc(II) metal-organic framework and its lanthanide(III) post-functionalizations, Dyes Pigments 159 (2018) 429–438.
[61] L. Li, J.-Y. Zou, S.-Y. You, H.-M. Cui, G.-P. Zeng, J.-Z. Cui, Tuning the luminescence of two 3d–4f metal–organic frameworks for the fast response and highly selective detection of aniline, Dalton Trans. 46 (47) (2017) 16432–16438.
[62] X.-L. Chen, L. Shang, L. Liu, H. Yang, H.-L. Cui, J.-J. Wang, A highly sensitive and multi-responsive Tb-MOF fluorescent sensor for the detection of Pb2+, Cr2O72−, B4O72−, aniline, nitrobenzene and cefixime, Dyes Pigments 196 (2021), 109809.
[63] B. Wang, R. He, L.-H. Xie, Z.-J. Lin, X. Zhang, J. Wang, H. Huang, Z. Zhang, K. S. Schanze, J. Zhang, S. Xiang, B. Chen, Microporous hydrogen-bonded organic framework for highly efficient turn-up fluorescent sensing of aniline, J. Am. Chem. Soc. 142 (28) (2020) 12478–12485.
[64] E. Teknikel, C. Unaleroglu, 2,3,5,6-Tetrabromo-8-phenyl BODIPY as a fluorometric and colorimetric probe for amines, J. Photochem. Photobiol. Chem. 422 (2022), 113549.
[65] S.W. Jaros, J. Sokolnicki, A. Wołoszyn, M. Haukka, A.M. Kirillov, P. Smoleński, A novel 2D coordination network built from hexacopper(i)-iodide clusters and cagelike aminophosphine blocks for reversible "turn-on" sensing of aniline, J. Mater. Chem. C 6 (7) (2018) 1670–1678.
[66] D.R. Lide, CRC Handbook of Chemistry and Physics, 85th Edition, 2004.
[67] J.E.F. Reynolds, Martindale: the Extra Pharmacopoeia, 31st ed., Royal Pharmaceutical Society, London, England, 1996.
[68] L. Zhang, C. Zhu, C. Chen, S. Zhu, J. Zhou, M. Wang, P. Shang, Determination of kanamycin using a molecularly imprinted SPR sensor, Food Chem. 266 (2018) 170–174.
[69] E. Adams, J. Dalle, E. De Bie, I. De Smedt, E. Roets, J. Hoogmartens, Analysis of kanamycin sulfate by liquid chromatography with pulsed electrochemical detection, J. Chromatogr. A 766 (1) (1997) 133–139.
[70] Y. Tao, D. Chen, H. Yu, L. Huang, Z. Liu, X. Cao, C. Yan, Y. Pan, Z. Liu, Z. Yuan, Simultaneous determination of 15 aminoglycoside(s) residues in animal derived foods by automated solid-phase extraction and liquid chromatography–tandem mass spectrometry, Food Chem. 135 (2) (2012) 676–683.
[71] Y.-F. Lin, Y.-C. Wang, S.Y. Chang, Capillary electrophoresis of aminoglycosides with argon-ion laser-induced fluorescence detection, J. Chromatogr. A 1188 (2) (2008) 331–333.
[72] X. Wang, M. Zou, X. Xu, R. Lei, K. Li, N. Li, Determination of human urinary kanamycin in one step using urea-enhanced surface plasmon resonance light-scattering of gold nanoparticles, Anal. Bioanal. Chem. 395 (7) (2009) 2397–2403.
[73] M. Ramezani, N.M. Danesh, P. Lavaee, K. Abnous, S.M. Taghdisi, A selective and sensitive fluorescent aptasensor for detection of kanamycin based on catalytic recycling activity of exonuclease III and gold nanoparticles, Sensor. Actuator. B Chem. 222 (2016) 1–7.
[74] P. Qin, B.A. Day, S. Okur, C. Li, A. Chandresh, C.E. Wilmer, L. Heinke, VOC mixture sensing with a MOF film sensor array: detection and discrimination of xylene isomers and their ternary blends, ACS Sens. 7 (6) (2022) 1666–1675.
[75] G. Gabrieli, R. Hu, K. Matsumoto, Y. Temiz, S. Bissig, A. Cox, R. Heller, A. López, J. Barroso, K. Kaneda, Y. Orii, P.W. Ruch, Combining an integrated sensor array with machine learning for the simultaneous quantification of multiple cations in aqueous mixtures, Anal. Chem. 93 (50) (2021) 16853–16861.
[76] D. Svechkarev, M.R. Sadykov, L.J. Houser, K.W. Bayles, A.M. Mohs, Fluorescent sensor arrays can predict and quantify the composition of multicomponent bacterial samples, Front. Chem. 7 (2020).
[77] K.J. Johnson, S.L. Rose-Pehrsson, Sensor array design for complex sensing tasks, Annu. Rev. Anal. Chem. 8 (1) (2015) 287–310.